Proc. Natl. Acad. Sci. USA
Vol. 74, No. 7, pp. 3068–3072, July 1977
Neurobiology

Nonlinear analysis of cat retinal ganglion cells in the frequency domain

(neural networks/vision)

JONATHAN D. VICTOR, ROBERT M. SHAPLEY, AND BRUCE W. KNIGHT

The Rockefeller University, New York, New York 10021

Communicated by Floyd Ratliff, April 13, 1977

ABSTRACT **We have analyzed the responses of cat retinal ganglion cells to luminosity gratings that are modulated in time by a sum of sinusoids. A judicious choice of the component temporal frequencies permits a separation of the linear and second-order nonlinear components. Y cell responses show harmonic generation and intermodulation distortion over a wide frequency range. These nonlinear components predominate over the linear components for certain types of spatial stimuli. Nonlinear components in X cells are greatly diminished in comparison. The character of the nonlinear responses provides strong constraints on prospective models for the nonlinear pathway of the Y cell.**

The visual pathway of the cat has been studied intensively in order to discover the stages in which the visual image undergoes neural transformation. Analyses of responses in retinal ganglion cells have led to the discovery of parallel processing in the cat retina (1). Distinct classes of ganglion cells, named X cells and Y cells, combine light-evoked signals from the receptors in different ways.

Previous studies in this laboratory provided evidence for the hypothesis that Y cells are excited by an ensemble of nonlinear spatial subunits (2, 3). Y cell receptive fields also have linear center and surround mechanisms. The linear and nonlinear mechanisms that drive the Y cell do not have similar spatial properties. This was demonstrated with the use of sinusoidally modulated spatial sine gratings as a visual stimulus. The linear mechanisms dominate the Y cell's response to gratings of low spatial frequency while the nonlinear subunits are the dominant input when the grating has a high spatial frequency. We have also found evidence that the linear and nonlinear mechanisms overlap extensively in the receptive field of the ganglion cell (3).

This paper reports on further studies of the nonlinearity in Y retinal ganglion cells of the cat with a new technique for nonlinear systems analysis. From the response to a grating that is amplitude-modulated by a sum of several sinusoids, we can derive a joint frequency response to pairs of input modulation frequencies. This joint response (or frequency kernel), $K(f_1,f_2)$, is susceptible to easy intuitive interpretation. It is also closely related to the Fourier transform of the second-order Wiener kernel (4).

The frequency kernel $K(f_1,f_2)$ represents the amount of nonlinear response produced by the system due to the presence of two sinusoids at the frequencies f_1 and f_2. For a linear system, $K(f_1,f_2) = 0$. We have used the kernel as a concise characterization of the dynamics of the nonlinear retinal pathway and as a clue to the nature of the nonlinearity. The linear frequency responses and second-order frequency kernels of X and Y cells have certain qualitative features that must be shared by any model for the retinal network. These features allow us to reject several simple models.

METHODS

Our experimental methods for recording from optic tract fibers have been described in detail (2). The visual stimulus was a spatial pattern of light modulated in time. A raster was formed on a cathode ray tube by sweep and triangle wave circuits. Its mean luminance was 20 cd/m^2, and its area was 20° × 20°. Synchronized to the sweep was a pattern waveform from a function generator; in these experiments the pattern was a sine grating. The pattern waveform was modulated in time by multiplying it by a relatively slow modulation signal produced by the computer. This produced a spatial pattern whose contrast changed with time (cf. ref. 5). If I_{max} is the maximum intensity on the screen and I_{min} is the minimum intensity, then the definition of contrast is:

$$(I_{max} - I_{min})/(I_{max} + I_{min}).$$

The modulation signal used in these experiments was a periodic signal composed of the sum of several sinusoids. The use of this signal in nonlinear systems analysis was an innovation suggested by Spekreijse's technique (6). The sum was formed by either six or eight sinusoids that spanned five to seven octaves. The component sinusoids were equal in amplitude in each episode. In different episodes, the amplitudes of the components were set to produce peak contrasts from 0.0125 up to 0.1 per sinusoid.

This modulation signal was chosen because (*i*) its values are distributed approximately as a Gaussian distribution, (*ii*) it has a power spectrum that spans a broad frequency band, and (*iii*) the discreteness of the input frequencies leads to a corresponding discreteness in the output frequencies, and this allows digital filtering of frequency-response components. When this modulation signal is used, one observes the effect of nonlinearities by measuring components in the response at harmonics and at combination frequencies. Linear transductions would yield only responses at the input set of frequencies, f_i. A quadratic nonlinearity would also produce response components at frequencies $f_i \pm f_j$ if f_i and f_j were frequencies in the input sinusoidal sum.

This technique requires a judicious choice of input frequencies. An inappropriate choice could lead to ambiguities that would obscure the dynamics of the nonlinear network under study. For instance, if the input frequencies were chosen so that $f_2 - f_1 = f_3 - f_2$, then the amplitude of the output at this mixture frequency would come from separate sources of intermodulation. If there are N input frequencies, then they must be chosen so that one can resolve the following N^2 combination frequencies: N second harmonics, $\frac{1}{2}N(N-1)$ sum frequencies, and $\frac{1}{2}N(N-1)$ difference frequencies. These frequencies must also be distinct from the N fundamental re-

sponse frequencies, f_i. We used several frequency sets that satisfied this condition. Expressed as multiples of 1/65.536 Hz, the sets were {42,72,162,352,802,1402}, {14,30,62,126, 254,510,1022,2046}, and {15,31,63,127,255,511,1023,2047}. The six-frequency set covered the range 0.6–21 Hz; the eight-frequency sets covered the range 0.2-30 Hz. In each set, successive frequencies were separated by about an octave.

Because all fundamental and second-order response frequencies were distinct, Fourier analysis of the nerve impulse train sufficed to determine each of the fundamental and second-order response components. The second-order response to each pair of input frequencies f_1 and f_2 appeared at a separate pair of output frequencies $f_1 \pm f_2$. The amplitude and phase shift measured at each of these output frequencies defined a single value of the experimentally determined second-order frequency kernel. The amplitude and phase at $f_1 + f_2$ defined the value of $K(f_1,f_2)$; the amplitude and phase at $f_1 - f_2$ defined the value of $K(f_1,-f_2)$.

Contour maps of the amplitude of the second-order frequency kernel $K(f_1,f_2)$ were constructed in the following way. Cartesian coordinates were chosen that were proportional to the logarithm of the frequencies f_1 and f_2 over the range of the input frequencies. In the range from zero to the lowest frequency used, the Cartesian coordinates were made linear. The laboratory measurements furnished values of the amplitude of $K(f_1,f_2)$ at discrete points within this two-dimensional coordinate system. The measurements at (f_1,f_1) should be multiplied by 2 for combinatorial reasons, and this has been done in all the graphs of frequency kernels in this paper. In principle, the values on the line $f_2 = -f_1$ are not measurable. Therefore, they were approximated by averaging neighboring values. The values of the amplitude at all other points where there was no experimental evaluation were interpolated by a standard two-dimensional cubic spline procedure. On theoretical grounds, the amplitude of $K(f_1,f_2)$ remains unchanged if f_1 and f_2 are either interchanged or else are both changed in signature. Because of this symmetry the behavior of the amplitude over the entire plane is determined by its behavior within the wedge between the lines $f_2 = f_1$ and $f_2 = -f_1$. For easier interpretation, the contour maps were plotted on the full right half plane. Thus, there are two lines of reflection: one runs diagonally through the upper half of the graph at $f_2 = f_1$ (the second harmonic diagonal), and the other runs diagonally through the lower half of the graph at $f_2 = -f_1$ (the zero frequency diagonal).

Relation to Wiener Analysis. The second-order frequency kernel is closely related to the Fourier transform of the second-order Wiener kernel (4). This is important because one can easily calculate the Wiener kernels of simple nonlinear models. Then, one can compare our measured frequency kernels with these theoretical predictions. If the system under study has no response components beyond first-order (linear) and second-order, the correspondence between our frequency kernel and the Wiener frequency kernel is exact. If the system does have higher-order response components, then our second-order frequency kernel contains contributions from Wiener frequency kernels of higher order. If the input frequencies were infinite in number and incommensurate, these higher-order contributions would vanish. On theoretical grounds, six or eight is a large enough number of sinusoids of incommensurate frequency to make higher-order contributions to the second-order frequency kernel negligible. The fact that we used sinusoids with commensurate frequencies results in a deviation of another kind: some higher-order combination frequencies of the input frequencies must coincide with the second-order frequencies. This problem can be countered by presenting the input sinusoids with different relative phases and appropriately averaging the second-order responses. This procedure yields a frequency kernel that is extremely close to the Fourier transform of the second-order Wiener kernel. Therefore, we can compare theoretical predictions for Wiener kernels of several simple models with our experimental data. (Details on the above considerations will be published separately.)

Presentation of input sinusoids with different relative phases is especially efficient when one uses the eight-frequency sets mentioned above. With these sets, all coincidences of higher-order response frequencies with second-order response frequencies are consequences of the identity

$$(2^j - 1) - 2(2^{j-1} - 1) = (2^k - 1) - 2(2^{k-1} - 1).$$

We used a scheme in which the eight frequencies were presented with eight different sets of relative phases. The relative phases were determined by a Hadamard matrix (7) by means of the following algorithm. An entry a_{ij} of +1 denotes that the ith sinusoid was presented with its maximum at time zero in the jth episode; an entry of −1 denotes that the sinusoid was presented with its minimum at time zero. A higher-order response component and a coincident second-order component have different dependences on the phases of the input sinusoids. For certain Hadamard matrices, each fourth- and sixth-order component has no net effect on a coincident second-order component because the phases will reinforce in four episodes and cancel in four episodes. Furthermore, all odd-order response frequencies are distinct from all even-order response frequencies. Thus, the lowest-order response frequencies whose effects on a second-order response frequency are not cancelled are those of order eight.

RESULTS

So far, we have studied 30 Y cells and 10 X cells in 15 cats. Each ganglion cell was mapped on a tangent screen and classified as X or Y by the following method. A sinusoidal grating, of high enough spatial frequency that it was just resolvable by the cell, was positioned in the center of the receptive field. This grating underwent periodic contrast reversal in time. Cells that responded at the fundamental frequency of the modulation were called X; cells that responded at the second harmonic of the modulation were classified as Y. In addition, the X cell response depended strongly on the spatial phase of the grating, exhibiting a sharp null for some particular spatial phase. The second harmonic response of the Y cell was independent of the spatial phase of a just-resolvable grating (cf. ref. 2).

The temporal modulation signal was then changed to the computer-generated sinusoidal sum. The computer recorded the times of nerve impulse occurrences for a series of presentations of the grating stimulus. For each cell, we explored a range of spatial frequencies, spatial phases, and contrasts.

The linear response amplitudes and the second-order frequency kernels obtained by Fourier analysis of the neural responses are shown graphically in the contour maps of Fig. 1 for representative X and Y cells. The contour maps show the response at second-order combination frequencies, $f_i \pm f_j$. Results for sum frequencies $(f_i + f_j)$ are in the upper half of each graph and for difference frequencies $(f_i - f_j)$ in the lower. The measured response amplitudes were reproducible to within about 1 impulse per sec on replicate runs. Thus, features of the frequency kernel that are distinguished by just one contour line are not significant.

The responses illustrated in Fig. 1 were elicited with a 0.5-cycle per degree (c/d) sinusoidal grating positioned to maximize

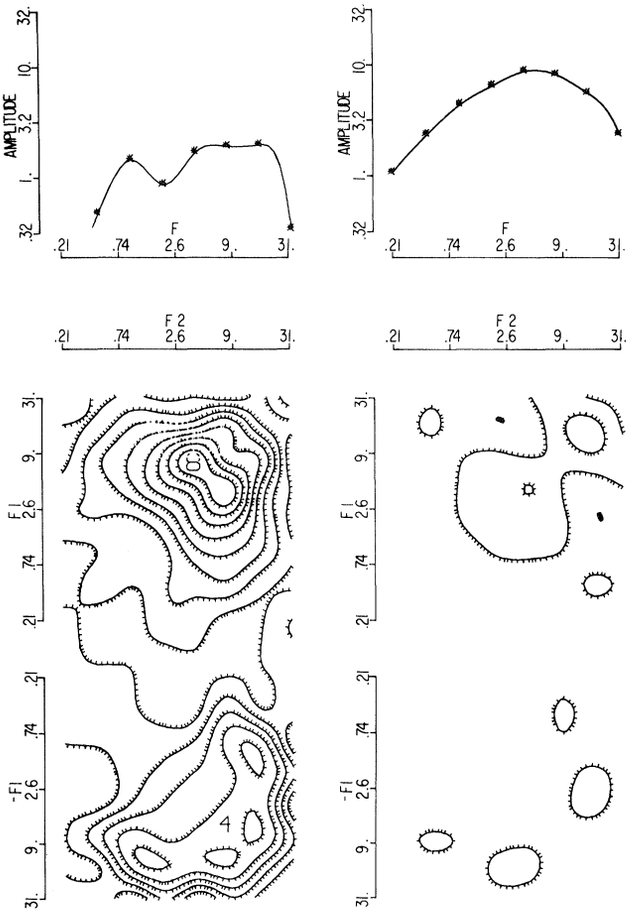

FIG. 1. Linear response and second-order frequency kernels obtained from a typical Y cell (*Left*) and a typical X cell (*Right*). The spatial pattern was a 0.5-cycle/degree sinusoidal grating in a position that produced a maximal linear response. The temporal modulation signal was the sum of eight sinusoids, each with a peak contrast of 0.05. Each contour line represents 1 impulse per sec; the tick-marks point downhill. Frequency is measured in Hz.

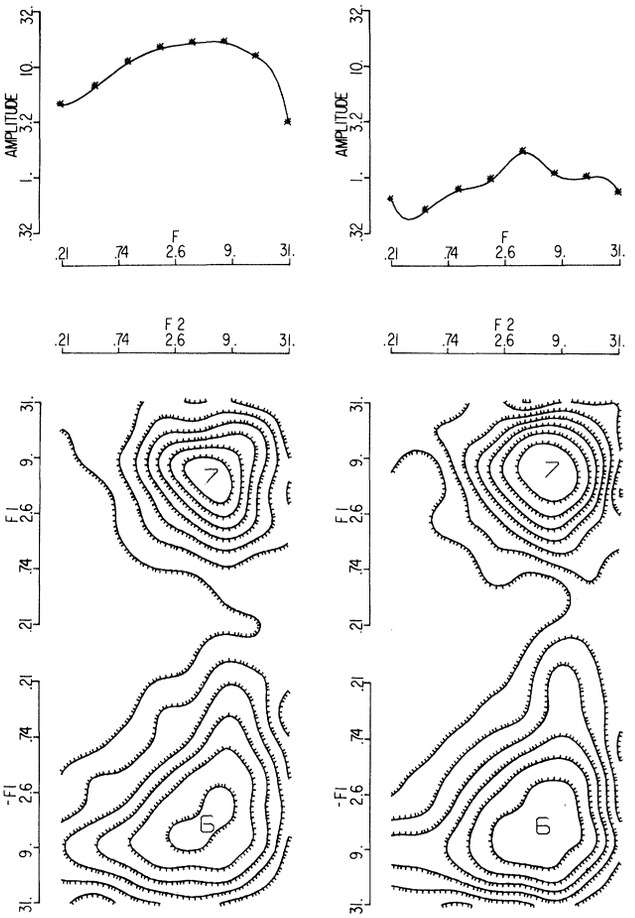

FIG. 2. Linear responses and second-order frequency kernels obtained from a Y cell with a 0.25-c/d grating. (*Left*) Grating positioned to produce a maximal linear response. (*Right*) Grating positioned to produce a minimal linear response. The temporal modulation was a sum of eight sinusoids, each with a peak contrast of 0.05. Each contour line represents 1 impulse per sec; the tick-marks point downhill. Frequency is measured in Hz.

the fundamental response. The temporal signal was a sum of eight sinusoids, each producing a peak contrast of 0.05. An average over eight relative phases of the input sinusoids was performed, as described under *Methods*. The Y cell's largest linear response was less than 2 impulses per sec. However, the frequency kernel had a large amplitude for many of the second-order combination frequencies. Both pure second harmonics ($2f_i$) and intermodulation frequencies ($f_i \pm f_j$) were present in the impulse train. The peak second-order frequency response was more than 8 impulses per sec near the diagonal $f_1 = f_2$ at an input frequency of about 6 Hz. The largest response at a second-order difference frequency was about 5 impulses per sec, at a somewhat higher input frequency. Clearly, the second-order response components dominated this neuron's response. A nearby X cell had a peak linear response of 16 impulses per sec to the input frequency near 8 Hz. All of the secord-order response components elicited from this cell were 2 impulses per sec or less.

In general, Y-type cat retinal ganglion cells have substantial response components at most sum and difference frequencies. The second-order frequency kernel typically peaked between 5 and 10 Hz on the input. The peak in the sum frequency spectrum lay on or near the diagonal $f_1 = f_2$. The difference frequency components differ significantly from the corresponding sum frequency components. The X-type retinal ganglion cells had substantially smaller second-order nonlinear response components under all stimulus conditions when compared with Y cells. Over a wide range of spatial frequencies of the pattern waveform, the linear response components of X cells dominated the total neural response.

The responses of Y cells at low spatial frequencies (typically 0.5 c/d or less) had substantial linear and second-order components. It was always possible to find a spatial phase of the grating, the null position, at which the linear responses became negligible. The second-order frequency kernel was virtually independent of spatial phase for moderate contrasts. This finding is illustrated in Fig. 2. A 0.25-c/d grating was presented, in alternate episodes, either in a position that produced a maximum linear response or at the null position. A sinusoidal sum composed of eight sinusoids, each producing a peak contrast of 0.1, formed the temporal modulation. An average over the relative phases of the input sinusoids was performed. The linear responses in the peak position of the grating were more than 7 impulses per sec to two of the input frequencies; at the null position, the linear responses were indistinguishable from noise. Nevertheless, the second-order frequency kernels recorded in the two positions were nearly identical. At sufficiently high contrasts, the fundamental response may be so large as to produce second-order components by truncation. In this case, one would expect a small dependence of the second-order

frequency kernel on spatial phase. In other Y cells, this effect has been observed.

DISCUSSION

The following results are useful for the formulation of theoretical models of the retina. (*i*) There is a clear qualitative distinction between X and Y cells in the amplitudes of their second-order frequency kernels. (*ii*) The Y cell nonlinearity produces substantial intermodulation responses as well as the second harmonics previously reported (2). (*iii*) There is a significant difference between responses at sum frequencies ($f_i + f_j$) and responses at difference frequencies ($f_i - f_j$). (*iv*) At peak and null positions for the fundamental frequency responses, the second-order frequency kernels were practically identical, providing strong evidence that the linear and nonlinear pathways are parallel. (*v*) Second harmonic responses of Y cells are approximately proportional to peak contrast. [This result has been reported before (cf. ref. 3) and we confirmed it in experiments in which a single sinusoid was used to modulate a sine grating of high spatial frequency.] The background luminance used in the present series of experiments (20 cd/m^2) was 20 times higher than used previously, yet the result was the same.

With these results it is possible to test models of the nonlinear pathway in the cat retina. Initially, we will consider the nature of the nonlinearity in the pathway that projects to Y cells, and then we will discuss models for the sequence of linear and nonlinear stages in this pathway.

Nature of Nonlinearity. The first class of nonlinearity one might consider is of the "operating point" type. One might suppose that the system is linear for small perturbations about an operating point but, as the input amplitude grows, the system's behavior is described by a segment of a nonlinear operating curve. Examples are fractional exponent power functions, logarithmic nonlinearities, and soft saturations. This hypothesis predicts that the amplitude of the second-order nonlinearity should decrease quadratically to zero as input amplitude goes to zero. This contradicts the observation that second harmonic responses scale less than quadratically (in fact, proportionally) with contrast. Another hypothesis destroyed by the same data is that the nonlinear element is a pure square law device.

A possibility not ruled out is that the nonlinearity resembles that of a rectifier of some kind (cf. ref. 3). The data imply that such a rectifier has a singularity at or near zero contrast and has an output proportional to contrast up to contrasts of about 0.15 or 0.20 and then saturates rapidly. We cannot yet determine whether this hypothetical rectifier is symmetric (like a full-wave rectifier) or asymmetric (like a half-wave rectifier).

If the nonlinearity of a system is of the "operating point" type, it makes sense to analyze that system by a best-approximating linear system, a best-approximating second-order nonlinear system, a best-approximating third-order nonlinear system, and so on. This is the approach carried out by Marmarelis and Naka (8, 9), who have investigated operating point nonlinearities in catfish retinal cells. For these nonlinear systems, the magnitudes of the nonlinear response components are small compared to the linear component and become vanishingly small as the input amplitude is reduced. However, we have shown that the cat Y cell nonlinearity is *not* of the operating point type. Therefore, one expects that the order-by-order modelling might not be useful in this case. Other examples exist of systems that are so highly nonlinear that they cannot be treated as operating point nonlinearities. For instance, Naka and his colleagues (9) found that Wiener analysis had to be carried to third order to obtain only passable agreement with the responses of the "transient" type of catfish amacrine cell. We have abandoned the order-by-order analysis. Instead, we formulate nonlinear models and test them on some of the features of the second-order frequency kernels. The sinusoidal sum is close enough to Gaussian noise to enable us to test predictions derived from the Wiener theory. The models we have tested are static nonlinearities preceded, or followed, or preceded and followed by linear filters.

Models for Y Cell Nonlinear Pathway. One possible hypothesis is that the ganglion cell receives a linear transformation of the input signal but, because its firing rate is bounded below by zero, nonlinear responses are produced by clipping. Various arguments dispose of this hypothesis, but perhaps the simplest is that, when the pattern waveform is a grating with a high spatial frequency, Y cells produce significant second-order frequency responses in the absence of linear frequency responses.

Somewhat more generally, one might imagine that the ganglion cell applies some other static nonlinearity at the level of impulse generation. For Gaussian inputs, this would imply that the second-order frequency kernel is $K(f_1,f_2) = c\,F(f_1)\,F(f_2)$ in which F is the frequency response of the linear transducer preceding the nonlinearity and c depends on the shape of this nonlinearity and on the input spectrum. [An equivalent formula has been stated elsewhere (8) and an outline of a proof is given below.]* In particular, the form above implies that $|K(f_1,f_2)| = |K(f_1,-f_2)|$. This prediction contradicts our third result—that the response amplitudes for difference frequencies depart from those at the corresponding sum frequencies.

Another possibility is that a static nonlinearity is present at the input to an otherwise linear system. This predicts $K(f_1,f_2) = c'G(f_1 + f_2)$ in which c' is again a scaling factor and G is the linear frequency response of the stages following the nonlinearity.* Our data disprove this hypothesis too; along a curve of constant $f_1 + f_2$, the frequency kernel has a prominent dip in amplitude where either f_1 or f_2 is small.

The simplest model that is not excluded immediately by the qualitative features of the frequency kernels is a sandwich composed of a static nonlinearity between two linear stages. One predicts that, for Gaussian inputs, $K(f_1,f_2) = c''F(f_1)\,F(f_2)\,G(f_1 + f_2)$ in which c'' is a scaling factor, F is the frequency response of the linear element that precedes the static nonlinearity, and G is the frequency response of the linear element that follows.* We have compared the second-order frequency kernel of Y cells with that of the best-fitting linear-nonlinear-linear sandwich model. At any given contrast, there is good qualitative agreement of the major features. Response components typically match to within 2 impulses per sec. Although a "sandwich model" is adequate for one contrast level, the shapes of the frequency kernels and the phases of the component responses change with contrast. This suggests that the elements of the sandwich must be considered to have a parametric dependence on contrast, and so a simple linear-nonlinear-linear sandwich model is also inadequate to account for our results. Even though the simple sandwich model must be rejected, we think that it may serve as the core of a more elaborate model that can account for the second-order frequency kernels at all contrasts. Models that are undergoing testing include

* These formulas may be verified as follows. First decompose the static nonlinear element into a parallel series of static devices, each of which corresponds to an appropriately normalized Hermite polynomial. Only the second Hermite polynomial contributes to the second-order Wiener kernel. For this purely quadratic subsystem, a simple calculation yields the desired result.

feedforward or feedback shunting inhibition (10, 11) adorning the simple sandwich model.

The resemblance between the highly layered morphology of the retina and the serial cascade of transducers in the "sandwich model" gives us hope that it may be possible to devise a unified model that will be consistent with anatomy and dynamics. The serial stages of tranductions in the nonlinear model of a cat Y cell might be related to the chain of connections that lead from bipolar cells to ganglion cells. From our work on X cells, and from the work by Marmarelis and Naka (8) on the catfish retina, it is plausible to think that photoreceptors and bipolar cells are approximately linear. These cells may be identified with the linear filter that precedes the nonlinearity. We guess that the nonlinearity resides in one of the types of amacrine cells. The filter after the nonlinearity may be related to the characteristic amacrine cell synapses that feed back onto bipolar cells and other amacrines.

We thank Dr. William Scott of Hoffmann-LaRoche for the gift of diallylbis-nortoxiferine used in the experiments. This work was supported by Grants EY188, EY1428, and EY1472 from the National Eye Institute.

The costs of publication of this article were defrayed in part by the payment of page charges from funds made available to support the research which is the subject of the article. This article must therefore be hereby marked "advertisement" in accordance with 18 U. S. C. §1734 solely to indicate this fact.

1. Enroth-Cugell, C. & Robson, J. G. (1966) "The contrast sensitivity of retinal ganglion cells of the cat," *J. Physiol. (London)* **187,** 517–552.
2. Hochstein, S. & Shapley, R. M. (1976) "Quantitative analysis of retinal ganglion cell classifications," *J. Physiol. (London)* **262,** 237–264.
3. Hochstein, S. & Shapley, R. M. (1976) "Linear and nonlinear spatial subunits in Y cat retinal ganglion cells," *J. Physiol. (London)* **262,** 265–284.
4. Wiener, N. (1958) *Nonlinear Problems in Random Theory* (The Technology Press of M.I.T. and Wiley, New York).
5. Shapley, R. M. & Rossetto, M. (1976) "An electronic visual stimulator," *Behav. Res. Methods Instrum.* **8,** 15–20.
6. Spekreijse, H. & Oosting, H. (1970) "Linearizing: A method for analyzing and synthesizing nonlinear systems," *Kybernetik* **7,** 22–31.
7. Beauchamp, K. G. (1975) *Walsh Functions and their applications.* (Academic Press, London, New York, San Francisco), p. 24
8. Marmarelis, P. & Naka, K. (1973) "Nonlinear analysis and synthesis of receptive field responses in the catfish retina II. One input white noise analysis," *J. Neurophysiol.* **36,** 619–633.
9. Naka, K., Marmarelis, P. & Chan, R. (1975) "Morphological and functional identifications of catfish retinal neurons III. Functional identification," *J. Neurophysiol.* **38,** 92–131.
10. Furman, G. G. (1965) "Comparison of models for subtractive and shunting lateral inhibition in receptor-neuron fields," *Kybernetik* **2,** 257–274.
11. Fuortes, M. G. F. & Hodgkin, A. L. (1964) "Changes in time scale and sensitivity in the ommatidia of *Limulus*," *J. Physiol. (London)* **172,** 239–263.